**Atmospheric
Measurement
Techniques
Discussions**

Evaluating calibration strategies for isotope ratio infrared spectroscopy for atmospheric $^{13}CO_2/^{12}CO_2$ measurement

X.-F. Wen[1], Y. Meng[1], X.-Y. Zhang[1], X.-M. Sun[1], and X. Lee[2,3]

[1]Key Laboratory of Ecosystem Network Observation and Modeling, Institute of Geographic Sciences and Natural Resources Research, Chinese Academy of Sciences, Beijing, 100101, China
[2]Yale-NUIST Center on Atmospheric Environment, Nanjing University of Information Science & Technology, Nanjing, 210044, China
[3]School of Forestry and Environmental Studies, Yale University, New Haven, Connecticut, 06511, USA

Correspondence to: X.-F. Wen (wenxf@igsnrr.ac.cn) and X. Lee (xuhui.lee@yale.edu)

Title Page

Abstract | Introduction

Conclusions | References

Tables | Figures

|◄ | ►|

◄ | ►

Back | Close

Full Screen / Esc

Printer-friendly Version

Interactive Discussion

Abstract

Isotope ratio infrared spectroscopy (IRIS) provides an in-situ technique for measuring $\delta^{13}C$ in atmospheric CO_2. A number of methods have been proposed for calibrating the IRIS measurements, but few studies have systematically evaluated their accuracy for atmospheric applications. In this study, we carried out laboratory and ambient measurements with two commercial IRIS analyzers and compared the accuracy of four calibration strategies. We found that calibration based on the ^{12}C and ^{13}C mixing ratios (Bowling et al., 2003) and that based on linear interpolation of the measured delta using the mixing ratio of the major isotopologue (Lee et al., 2005) yielded accuracy better than 0.06 ‰. Over a 7-day atmospheric measurement in Beijing, the two analyzers differed by 9.44 ± 1.65 ‰ (mean ± 1 standard deviation of hourly values) before calibration and agreed to within -0.02 ± 0.18 ‰ after properly calibration. However, even after calibration the difference between the two analyzers showed a slight correlation with concentration, and this concentration dependence propagated through the Keeling analysis resulting in a much larger difference of 2.44 ‰ for the Keeling intercept. The high sensitivity of the Keeling analysis to the concentration dependence underscores the challenge of IRIS for atmospheric research.

1 Introduction

Isotope ratio infrared spectroscopy (IRIS) is an emerging technology for making in-situ, continuous $\delta^{13}C$ observation in ambient conditions. With proper calibration, it can achieve precision similar to that of isotope ratio mass spectrometry (IRMS) (Kerstel and Gianfrani, 2008; Berryman et al., 2011; Werner et al., 2012). At least five types of IRIS instruments are available for field measurement of $\delta^{13}C$, including tunable diode laser absorption spectroscopy (Campbell Scientific Inc., Logan, UT; e.g. Bowling et al., 2003; Griffis et al., 2008; Wingate et al., 2010; Santos et al., 2012), quantum cascade laser absorption spectroscopy (Aerodyne Research, Inc., Billerica, MA; e.g. Wada et al.,

2011; Kammer et al., 2011; Sturm et al., 2012), wavelength-scanned cavity ring-down spectroscopy (Picarro Inc., Sunnyvale, CA; e.g. Friedrichs et al., 2010; Bai et al., 2011; Berryman et al., 2011), off-axis integrated cavity output spectroscopy (Los Gatos Research, Mountain View, CA; e.g. McAlexander et al., 2011; Guillon et al., 2012), and Fourier transform infrared spectroscopy (e.g. Mohn et al., 2008; Griffith et al., 2012; Hammer et al., 2012). All the IRIS instruments should maintain accuracy traceable to the international PDB-CO_2 or VPDB-CO_2 scale. In comparison to IRMS, however, IRIS is a relatively immature technology still subject to a number of artifacts (Griffith et al., 2012; Werner et al., 2012). Sensibility to changing environmental conditions and dependence of $\delta^{13}C$ on CO_2 concentration are the two main sources of error affecting the IRIS measurements (Wada et al., 2011; McAlexander et al., 2011; Guillon et al., 2012). Proper calibration is necessary to ensure accurate measurements (Bowling 2003; Kammer et al., 2011; Guillon et al., 2012; Hammer et al., 2012; Vogel et al., 2012).

General speaking, the IRIS instrument calibration strategy consists of pre-deployment and in-deployment components. Predeployment calibration is implemented by altering the analyzer's internal parameter set, either by the manufacturer or by the user, prior to field deployment (e.g. Guillon et al., 2012; Sturm et al., 2012). Additional calibration is carried out during field deployment to remove instrument drift and the residual concentration dependence. In this study, the pre-deployment calibration performed at the factory was left intact; instead the focus was on the in-deployment calibration.

The four in-deployment calibration methods we have examined (Sect. 2.2) fall into the categories of both absolute and empirical calibration (e.g. Griffith et al., 2012). Briefly, in Method 1 the mixing ratios of the individual isotopologues are calibrated separately against two or more standard gases of known $^{12}CO_2$ and $^{13}CO_2$ mixing ratios (Bowling et al., 2003; Griffis et al., 2005; Wingate et al., 2010; Griffith et al., 2012). Method 2 removes the instrument drift and concentration dependence by interpolating the measured delta value using the mixing ratio of the major isotopologue; this method is used

in field measurements of water vapor isotopes (Lee et al., 2005; Wen et al., 2008, 2012; Welp et al., 2012) and has yet to be applied to $\delta^{13}C$ measurements Recommended by Picarro Inc., Method 3 is a variation to Method 2 whereby the interpolation is carried out using two or more delta values (Berryman et al., 2011; Wada et al., 2011; Vogel et al., 2012) to minimize the delta-stretching effect. Recommended by Los Gatos Inc. Method 4 corrects the measured delta with a single offset value and thus requiring only one calibration gas.

In this paper, we report the results of a performance evaluation on two commercial IRIS analyzers. Measurements were made in the laboratory and in ambient conditions. Calibration was carried out using the four methods described above. We wish (1) to evaluate the accuracy of these two analyzers, (2) to identify the most appropriate calibration strategy for atmospheric applications, and (3) to examine error propagation of the concentration dependence through the Keeling analysis.

2 Materials and methods

2.1 Analyzers and sampling configuration

The two IRIS analyzers used in this study were manufactured in 2010 by the Picarro Inc., Sunnyvale, CA (models G1101-i) and the Los Gatos Research Inc., Mountain View, CA (model DLT-100). The Picarro analyzer was upgraded in March 2012 to remove spectral contamination caused by CH_4.

The Picarro analyzer was configured with two three-way solenoid valves, resulting in one common port and three sample ports. The valves were controlled by the electric signal provided by the analyzer. The analyzer's sampling cell was maintained at a low pressure (140 torr) and constant temperature (45 °C). Gas was not dried before entering the analyzer. (The water dilution and pressure broadening effect were supposed to be corrected by firmware imbedded in the instrument. In our case, the correction coefficients supplied by the manufacturer were erroneous, resulting in too large corrections

on the pressure broadening effect. In the following, only correction to the water dilution effect was made.) The analyzer drew sampling air and calibration air at a flow rate of $0.03\,L\,min^{-1}$ STP and recorded the signals at 0.3 Hz.

The Los Gatos analyzer was coupled with a multi-inlet unit supplied by the manufacturer (model 908-0003-9002), which allowed automatic switching between 8 different sampling ports. Its sampling and calibration flow rate were $0.5\,L\,min^{-1}$ STP and its sampling cell was maintained at low pressure (38 torr) and constant temperature (45 °C). Gas was dried by passing through a Nafion gas dryer (PD-200T-12MPS, Perma Pure, Toms River, New Jersey) and then a drierite tube before entering the analyzer to prevent water absorption interference. All measurements were made at 1 Hz.

2.2 Calibration procedures

2.2.1 Method 1: two-point mixing ratio gain and offset calibration

Method 1 is described by Bowling et al. (2003), Griffis et al. (2005), and Griffith et al. (2012). Let x_i^{12} and x_i^{13} be the $^{12}CO_2$ and $^{13}CO_2$ volume mixing ratio and subscript i denote sampling sequence with $i = 1$, 2 and a standing for standard gas 1, standard gas 2 and sampling air, respectively. The calibration equations are

$$x_{a,t}^{12} = \frac{x_{2,t}^{12} - x_{1,t}^{12}}{x_{2,m}^{12} - x_{1,m}^{12}} \left(x_{a,m}^{12} - x_{1,m}^{12} \right) + x_{1,t}^{12} \qquad (1)$$

$$x_{a,t}^{13} = \frac{x_{2,t}^{13} - x_{1,t}^{13}}{x_{2,m}^{13} - x_{1,m}^{13}} \left(x_{a,m}^{13} - x_{1,m}^{13} \right) + x_{1,t}^{13} \qquad (2)$$

where the additional subscript t and m indicate the true and the un-calibrated mixing ratio, respectively.

This method requires standard gases of known mixing ratios of $[^{12}CO_2]$ and $[^{13}CO_2]$. These values are derived from of the known total $[CO_2]$ mixing ratio and the $\delta^{13}C$ values according to:

$$[CO_2]=[^{12}CO_2] + [^{13}CO_2] + f[CO_2] \tag{3a}$$

$$R_a = [^{13}C]/[^{12}C]=[^{13}CO_2]/[^{12}CO_2]=R_{VPDB}(1 + \delta_a/1000) \tag{3b}$$

$$[^{12}CO_2]=[CO_2](1-f)]/(1 + R_{VPDB}(1 + \delta_a/1000)) \tag{3c}$$

$$[^{13}CO_2]=[CO_2](1-f)-[^{12}CO_2] \tag{3d}$$

where $[CO_2]$ is the total mixing ratio including all CO_2 isotopomers, f is the fraction (0.00474) of CO_2 containing all isotopomers other than $^{13}C^{16}O_2$ and $^{12}C^{16}O_2$, and R_{VPDB} is the $^{13}C/^{12}C$ standard molar ratio, 0.0111797 (Vienna Peedee Belemnite or VPDB-CO_2 scale, i.e. reference material 8544, NBS19) (Allison et al., 1995).

The isotopic molar mixing ratio is converted to the delta notation as

$$\delta^{13}C= \left(R_{sample}/R_{VPDB}-1\right) \times 1000\text{‰} \tag{4}$$

where R is the ratio of ^{13}C to ^{12}C in the sample ($= x^{13}_{a,t}/x^{12}_{a,t}$).

2.2.2 Method 2: two-point mixing ratio interpolation

This method has been used for water vapor isotope measurements (Lee et al., 2005; Wen et al., 2008, 2012; Welp et al., 2012). An advantage of this method is that the isotope ratio of the standard gas should be known precisely (such as via IRMS analysis) but its mixing ratio does not need to. Its application to the $\delta^{13}C$ measurement consists of several steps. Using standard gas 1 as the span calibration gas, the calibrated carbon dioxide molar mixing ratio (^{13}C /^{12}C) is given by

$$R_{a,1} = R_1 \frac{x^{13}_{a,m}\, x^{12}_{1,m}}{x^{13}_{1,m}\, x^{12}_{a,m}} \tag{5}$$

where R_1 is the (known) ^{13}C/^{12}C ratio of standard gas 1. Similarly, using standard gas 2 as the span calibration gas, we have

$$R_{a,2} = R_2 \frac{x_{a,m}^{13} \, x_{2,m}^{12}}{x_{2,m}^{13} \, x_{a,m}^{12}} \qquad (6)$$

where R_2 is the (known) ^{13}C/^{12}C ratio of standard gas 2. The molar ratio of the carbon dioxide isotopologues in the sample, $R_{a,1}$ and $R_{a,2}$, are converted to the delta notation, $\delta_{a,1}$ and $\delta_{a,2}$ according to Eq. (4).

Next, a linear interpolation is made between the measured ^{12}C mixing ratio to find the true ambient isotope ratio

$$\delta_{a,t} = \frac{\left(\delta_{a,2} - \delta_{a,1}\right)}{\left(x_{2,m}^{12} - x_{1,m}^{12}\right)} \left(x_{a,m}^{12} - x_{1,m}^{12}\right) + \delta_{a,1} \qquad (7)$$

The mixing ratio measurements are calibrated using Eqs. (1)–(2).

2.3 Method 3: two-point delta value gain and offset calibration

Method 3 requires two standard gases with known but different $\delta^{13}C$. It assumes that the measured $\delta^{13}C$ of the standard gas is linearly dependent on its true $\delta^{13}C$ and independent on its mixing ratio (e.g. Vogel et al., 2012; Sturm et al., 2012). The calibration is given by

$$\delta_{a,t} = \delta_{a,m} \cdot m + b \qquad (8)$$

where

$$m = \frac{\delta_{1,t} - \delta_{2,t}}{\delta_{1,m} - \delta_{2,m}} \qquad (9)$$

$$b = \delta_{1,t} - \frac{\delta_{1,t} - \delta_{2,t}}{\delta_{1,m} - \delta_{2,m}} \delta_{1,m} \tag{10}$$

where δ_1 and δ_2 is the (true or measured) $\delta^{13}C$ of standard gas 1 and 2, respectively.

In the case that more than two standard gases are available, the coefficients m and b can be derived from linear regression.

As with Methods 1 and 2, the Eqs. (1)–(2) are used for calibration of the mixing ratio measurements.

2.3.1 Method 4: single-point delta value offset calibration

Method 4 requires a single standard gas (denoted by subscript 1) with known $\delta^{13}C$. The calibration equation is given by

$$\delta_{a,t} = \delta_{a,m} + (\delta_{1,t} - \delta_{1,m}) \tag{11}$$

Since in this case only one standard gas is available, the mixing ratio is calibrated using the following equations:

$$[CO_2]_{a,t} = \frac{[CO_2]_{1,t}}{[CO_2]_{1,m}} [CO_2]_{a,m} \tag{12}$$

2.4 Standard gases

Three standards gases (Std 1: 361.25 ppm for $[CO_2]$ and -8.909‰ for $\delta^{13}C$; Std 2: 398.76 ppm for $[CO_2]$ and -8.652‰ for $\delta^{13}C$; Std 3: 436.41 ppm for $[CO_2]$ and -10.134‰ for $\delta^{13}C$) were obtained from the Key Laboratory for Atmospheric Chemistry, Chinese Academy of Meteorological Sciences, China Meteorological Administration. The CO_2 concentrations of these gases are traceable to the WMO 2007 Scale at the Central Calibration Laboratory (CCL) of the World Meteorological Organization (WMO), and their $\delta^{13}C$ values are traceable to the NBS-19 and the NBS20 scale of the International Atomic Energy Agency and NOAA-EASL.

2.5 Laboratory tests

In the first test, the precision of the analyzers was determined by estimating the Allan deviations of the CO_2 concentration and the $\delta^{13}C$ value (Werle, 2011). Air sample was drawn continuously into the analyzers from a compressed air tank with $[CO_2]$ of 420 ppm and $\delta^{13}C$ of $-9.8\,‰$. Each measurement lasted 24 h.

In the second test, the three standard gases were measured sequentially. The switching sequence was Std 1, Std 2, Std 3, with 10 min spent on each intake. The first two minutes of each measurement were discarded because of the transient response to step change. The calibration was done using the above procedures for each switching cycle by treating one of the three gases as the target of measurement and the other two gases as the calibration standards, and hourly mean values were produced from the calibrated measurements. This test lasted 24 h for each analyzer.

2.6 Atmospheric measurement

A purpose of the atmospheric measurement was to assess how these calibration procedures impact the analyzers' ability to measure $\delta^{13}C$ in atmospheric CO_2. The data were also used to evaluate error propagation through the Keeling mixing line analysis. The analyzers drew ambient air through one sample intake from the outside of our laboratory in Beijing, China, from 12 to 18 April (DOY 103–109) in 2012. The intake lines of both analyzers were equipped with a filter (Swagelok model B-4F-05, Connecticut Valves and Fittings, Norwalk, Connecticut) contained in an enclosure heated to 60 °C to avoid condensation. The analyzers sampled gas standards Std 1 and Std 3 in the first 10 min of every hour, each lasting 5 min, and spent the remainder of the hour measuring the air sample. Calibration was carried out for each switching cycle, and hourly mean values were produced from the atmospheric measurements.

The isotope signal of CO_2 sources in Beijing was determined using the Keeling plot. The Keeling mixing model parameters were obtained from a geometric mean

regression of the carbon isotope ratio of ambient CO_2 versus the reciprocal of the total [CO_2] following the procedure outlined in Bowling et al. (2002) and Pataki et al. (2003).

3   Results and discussion

3.1   Precision of measurement

Figure 1 shows the time series of the $^{12}CO_2$ concentration and Allan deviation as a function of averaging time for the $^{12}CO_2$ mixing ratio and $\delta^{13}C$. The dashed lines show the expected behavior of the Allan deviation versus time for random noises. The $^{12}CO_2$ mixing ratio precision improves with increasing averaging time; the best precision of 0.013 and 0.016 ppm was obtained with about 1800 and 500 s averaging for the Picarro and the Los Gatos analyzers, respectively. The Picarro analyzer delta measurement had the best precision of 0.08 ‰ at 2000 s, and the Los Gatos analyzer had the best precision of 0.04 ‰ at 1000 s. For longer averaging times, the precision degraded because of instrumental drift. The averaging period for the laboratory test (600 s) and for the atmospheric measurement (3000 s) were slightly different than the optimal averaging length revealed by the Allan analysis.

Our precision values are typical of IRIS instruments for $\delta^{13}C$. For example, Friedrichs et al. (2010) showed a precision of 0.08 ‰ with 130 min averaging for a Picarro analyzer model EnviroSense 2050. Vogel et al. (2012) found a precision 0.2 ‰ with 5 min averaging intervals for a model G1101-i analyzer from Picarro. Guillon et al. (2012) and McAlexander et al. (2011) found a precision of 0.05 and 0.15 ‰ with 60 s averaging for two model DLT-100 analyzers from Los Gatos. Bowling et al. (2003) showed a precision of 0.25 ‰ with a 2 min sampling interval for a model TGA100 from Campbell Scientific. Wada et al. (2011) found a precision of 0.05 ‰ with an integration time of 10 s for an analyzer from Aerodyne Research.

3.2 Comparison of calibration methods

Table 1 summarizes the results of the four δ^{13}C calibration methods as applied to the Picarro and the Los Gatos measurements of the standard gases in the laboratory test. Without calibration the measured δ^{13}C values deviated from the true values by -1.79
5 to -2.22‰ for the Picarro analyzer and -4.33 to -5.70‰ for the Los Gatos analyzer.

The δ^{13}C error listed in Table 1 is defined as the calibrated delta minus the true delta after calibration using one of the four methods. In the case of Method 1, the error for standard gas 1 (Std 1) was obtained by calibrating its measurement against standards gases Std 2 and Std 3, and so on. The accuracy generally were better than 0.03‰ for
10 both analyzers. Slightly better accuracy and precision were obtained if the calibration was interpolation (for Std 2) than extrapolation (for Std 1 and Std 3). In agreement with the Allan variance analysis (Fig. 1b), the precision of the Los Gatos analyzer was better than that of the Picarro analyzer, although both analyzers had worse precision than the best Allan variance precision due to the slightly shorter (600 s) averaging length than
15 optimal calibration cycle.

The delta errors listed for Method 2 were obtained similarly to those for Method 1. For example, the error for standard gas 1 (Std 1) was obtained by calibrating its measurement against standards gases Std 2 and Std 3. The accuracy were generally better than 0.04‰ for the Picarro analyzer, which is nearly identical to the results of Method
20 1. The accuracy was not as good as that obtained with Method 1 for the Los Gatos analyzer. In addition, the error and precision of extrapolation were also worse than those of interpolation for both analyzers. Our results support the standard practice that the concentrations of the calibration gases should bracket the ambient concentration.

It should be pointed out that Method 1 requires that the CO_2 mixing ratio and δ^{13}C
25 of the calibration gases be known precisely, while Method 2 only requires that δ^{13}C be known. Calibration gases supplied by local vendors often have a concentration accuracy certified to 1 %; After their ^{13}C has been analyzed by IRMS, these gases can be used for Method 2 but may not be good enough for Method 1. For example, let

Title Page

Abstract | Introduction

Conclusions | References

Tables | Figures

|◄ | ►|

◄ | ►

Back | Close

Full Screen / Esc

Printer-friendly Version

Interactive Discussion

us suppose that the CO_2 concentration of Std 3 is biased high by 1 %. Interpolating with Std 1 and Std 3, the accuracy and precision of the Std 2 measurement after the Method 1 calibration would be 0.05 ± 0.30 ‰ and 0.06 ± 0.11 ‰ for the Picarro and the Los Gatos analyzer, respectively, which are slightly worse than those in Table 1. Extrapolating with Std 2 and (the biased) Std 3, the Std 1 measurement would have an accuracy and precision of -0.24 ± 0.73 ‰ and -0.26 ± 0.26 ‰ for the Picarro and the Los Gatos analyzers, respectively, which are much worse than those shown in Table 1.

Method 3 was applied to the measurement of standard gas 1 using standards Std 2 and Std 3 for calibration and to the measurement of standard gas 2 using standard Std 1 and Std 3 for calibration. Measurement errors for standard gas 3 were not quantified because the delta values of Std 1 and Std 2 were too close to each other as an effective calibration pair. The error was greater than 0.19 ‰ for the Picarro analyzer and 0.49 ‰ for the Los Gatos analyzer. We conclude that for these analyzers Method 3 was inferior to Methods 1 and 2.

Similarly, Method 4 was not recommended for these analyzers. The one-point delta offset correction (Eq. 11) using Std 3 as the calibration standard removed much of the measurement errors for standard gas 1 and 2. Still, the residual error was greater than 0.19 ‰ for the Picarro analyzer and 0.62 ‰ for the Los Gatos analyzer.

3.3 Comparison of the two analyzers

Figure 2 illustrates the time variations of atmospheric $\delta^{13}C$ in Beijing during DOY 103–109 (12 to 18 April) in 2012, the difference between the Picarro and the Los Gatos analyzers and a histogram of the differences. Here the results of Method 1 are shown. The analyzers observed similar diurnal cycles due to atmospheric entrainment and boundary layer mixing. No obvious systematic difference existed between the two analyzers with the difference being only -0.02 ± 0.18 ‰ (mean and standard deviation of hourly measurements). The difference can be approximated by the Gaussian distribution. If Method 2 was used for calibration, the mean difference was 0.03 ± 0.19 ‰.

Figure 3a illustrates the corresponding time variation of atmospheric CO_2 concentration and the difference between the two analyzers. Although similar diurnal cycles were observed the concentration measured by the Picarro analyzer was 2.2 ± 1.0 ppm lower than that of the Los Gatos analyzer. The difference was systematic and became larger as the H_2O concentration increased (Fig. 3b). Two factors may have contributed to the difference. The Nafion dryer and the drierite tube used by the Loa Gatos analyzer should yield an outlet dew point of lower than $-35\,°C$ or about 300 ppm of water vapor. The corresponding dilution effect is an underestimation of CO_2 concentration of 0.1 ppm at 400 ppm of carbon dioxide. In the case of the Picarro analyzer, as pointed out in Sect. 2.1, the correction coefficients supplied by the manufacturer were erroneous, resulting in too large corrections on the water vapor effect. We were able to correct the dilution effect using the water vapor concentration measured by the analyzer but was unable to remove the effect due to the water vapor pressure broadening and the HDO spectral interference (Rella et al., 2012a; Nara et al., 2012). These latter effects are on the order of 2 ppm for every 1 % increase in water vapor concentration at 400 ppm of carbon dioxide (Rella et al., 2012b).

Figure 4 shows the dependence of the difference of atmospheric $\delta^{13}C$ calibrated with Method 1 and that calibrated with Method 2 on the corresponding CO_2 concentration. No obvious concentration dependence was observed for the Picarro analyzer, but some dependence existed for the Los Gatos analyzer. It is not clear why the two calibration methods would yielded nearly identical results for one analyzer but not for the other.

Figure 5 also shows that the difference of the calibrated atmospheric $\delta^{13}C$ between the analyzers was also dependent on the CO_2 concentration. Once again, the results of Method 1 are shown. Even though the mean difference between two analyzers was very small (-0.02 ± 0.18‰), there was a slight negative linear relationship of the hourly $\delta^{13}C$ bias between the analyzers to the CO_2 concentration.

3.4 Error propagation in the Keeling mixing line analysis

Table 2 summarizes the results of the Keeling analysis of the atmospheric measurement using the four different calibration methods. Figure 6 gives the Keeling plot for the results obtained with the Method 1 calibration. The intercept of Keeling plot was -23.85 ± 1.00‰ ($\pm 95\%$ confidential level) for the Picarro analyzer, and -21.85 ± 0.79‰ for the Los Gatos analyzer, based on the results of Method 1 (Table 2).

If the analysis was restricted to the nighttime (22:00 to 04:00 LT) to better isolate the local influence, the intercept of Keeling plot was reduced to -25.53 ± 1.99‰ for the Picarro analyzer, and -23.81 ± 1.52‰ for the Los Gatos analyzer, based on the results of Method 1. The intercept during the nighttime represents the integrated value of the potential CO_2 sources in an urban airshed (Pataki et al., 2007; Wada et al., 2011), which should be a mixture of natural gas, gasoline and coal combustion and biogenic respiration of plants and soil. Our lab is next to the Beijing Olympic Garden dominated by trees and grasses, and domestic heating (by coal and natural gas) in Beijing ended on 18 March (DOY 78) in 2012. In general, the δ^{13}C values of C3 plants are in the range of -22 to -35‰, and that of C4 plants are in the range of -19 to -9‰ (Koch, 2008). Pataki et al. (2003) found a high degree of temporal and spatial variability in C3 ecosystems, with individual observations ranging from -32.6 to -19.0‰. Soil δ^{13}C values vary from -23.5 to -16.3‰ in the Dallas metropolitan area, Texas (Clark-Thorne and Yapp, 2003). The δ^{13}C values of natural gas combustion are in the range of -42 to -37‰, gasoline combustion in the range of -28 to -60‰, and coal in the range of -27 to -25‰ (Clark-Thorne and Yapp, 2003; Pataki et al., 2007; Wada et al., 2011). Our Keeling intercept values appeared to show that C4 reparation was important sources of the urban CO_2 in Beijing in addition to fossil combustion.

The intercept difference between the two analyzers (2.00‰, Method 1) was substantially larger than the difference between their δ^{13}C measurements (-0.02 ± 0.18‰; Fig. 2). We performed a sensitivity analysis in order to understand error propagation

of the concentration dependent behavior in the Keeling analysis. We assumed that the true atmospheric $\delta^{13}C$ is a linear function of the inverse of the CO_2 concentration, as given by the regression shown in Fig. 6a

$$\delta^{13}C = \frac{6133.3}{[CO_2]} - 23.85 \tag{13}$$

We then added a small concentration-dependent error to this equation

$$\delta^{13}C = \frac{6133.3}{[CO_2]} - 23.85 + d \tag{14}$$

where d is a parameter that describes the severity of the concentration dependence

$$d = -\varepsilon + \frac{2\varepsilon}{50}([CO_2] - 400) \tag{15}$$

In Eq. (15), the delta error is $-\varepsilon$ at a concentration of 400 ppm and $+\varepsilon$ at a concentration of 450 ppm. Finally we recomputed the y-intercept of Eq. (14) by varying ε. The results, given in Fig. 7, shows that the error propagation through the concentration dependence as a function of ε on the intercept of the Keeling plot.

The results in Fig. 7 can largely explain the intercept differences between the two analyzers. In the case of the difference seen between the two analyzers, the concentration dependence (Fig. 5) can be approximated by Eq. (15) with $\varepsilon = 0.15$‰. According to Fig. 7, this error would propagate through the Keeling analysis resulting in a difference of 2.44‰ in the Keeling intercept. This prediction was close to actual difference of 2.00‰ in the intercept value (Table 2).

Similarly, the uncertainty in the Keeling intercept caused by the calibration method can be understood through the error propagation prediction. For the Picarro analyzer, there was no concentration dependence in the calibrated $\delta^{13}C$ between Methods 1 and 2, and the intercept values based on these two methods were nearly identical. In the case of the Los Gatos analyzer, the Keeling intercept was -21.85 ± 0.79‰ if Method

Title Page

Abstract | Introduction

Conclusions | References

Tables | Figures

◄ | ►|

◄ | ►

Back | Close

Full Screen / Esc

Printer-friendly Version

Interactive Discussion

1 was used for calibration, and $-20.62 \pm 0.79\,‰$ if Method 2 was used (even though the actual δ^{13}C differed by only $-0.5 \pm 0.05\,‰$; data not shown), giving a difference of $-1.23\,‰$ (Method 1–Method 2). The concentration dependence shown in Fig. 4 yielded a value of $-0.8\,‰$ for the parameter ε. According to Fig. 7, the concentration dependence would result in a difference of $-1.39\,‰$ for the Keeling intercept between the two methods.

4 Conclusions

In this study, an inter-comparison was made between one analyzer from Picarro Inc. (models G1101-i) and one analyzer from Los Gatos Research (model DLT-100) to characterize their performance, to compare different calibration strategies and to investigate error propagation of the concentration dependence through the Keeling analysis. We showed that the preferred calibration methods were that based on calibration of the ^{12}C and ^{13}C mixing ratio (Method 1) and that based on the delta interpolation using the measured ^{12}C mixing ratio. These methods yielded accuracy better than $0.06\,‰$ for the Picarro and Los Gatos analyzers. Over the 7-day atmospheric measurement, the two analyzers tracked the natural variability of δ^{13}C very well and achieved an average difference of $-0.02 \pm 0.18\,‰$.

We found that even a small concentration dependence can be amplified in the Keeling analysis causing large errors in the Keeling intercept. Even though the mean difference was small ($-0.02\,‰$), because the difference in the hourly delta value between the two analyzers was linearly correlated with the CO_2 concentration, a much larger difference of $2.44\,‰$ was found for the Keeling intercept.

References

Allison, C. A., Francey, R. J., and Meijer, H. A. J.: Recommendations for the reporting of stable isotope measurements of carbon and oxygen in CO_2 gas, Reference and intercomparison materials for stable isotopes of light elements, IAEA-TECDOC 825, Int. At. Energy Agency, Vienna, 155–162, 1995.

Bai, M., Köstler, M., Kunstmann, J., Wilske, B., Gattinger, A., Frede, H. G., and Breuer, L.: Biodegradability screening of soil amendments through coupling of wavelength-scanned cavity ring-down spectroscopy to multiple dynamic chambers, Rapid Commun. Mass Spectrom., 25, 3683–3689, 2011.

Berryman, E. M., Marshall, J. D., Rahn, T., Cook, S. P., and Litvak, M.: Adaptation of continuous flow cavity ring down spectroscopy for batch analysis of $\delta^{13}C$ of CO_2 and comparison with isotope ratio mass spectrometry, Rapid Commun. Mass Spectrom., 25, 2355–2360, 2011.

Bowling, D. R., McDowell, N. G., Bond, B. J., Law, B. E., and Ehleringer, J. R.: ^{13}C content of ecosystem respiration is linked to precipitation and vapor pressure deficit, Oecologia, 131, 113–124, 2002.

Bowling, D. R., Sargent, S. D., Tanner, B. D., and Ehleringer, J. R.: Tunable diode laser absorption spectroscopy for stable isotope studies of ecosystem–atmosphere CO_2 exchange, Agr. Forest Meteorol., 118, 1–19, 2003.

Clark-Thorne, S. T. and Yapp, C. J.: Stable carbon isotope constraints on mixing and mass balance of CO_2 in an urban atmosphere: Dallas metropolitan area, Texas, USA, Appl. Geochem., 18, 75–95, 2003.

Friedrichs, G., Bock, J., Temps, F., Fietzek, P., Körtzinger, A., and Wallace, D.: Toward continuous monitoring of seawater $^{13}CO_2/^{12}CO_2$ isotope ratio and pCO_2: Performance of cavity ringdown spectroscopy and gas matrix effects, Limnol. Oceanogr. Meth., 8, 539–551, 2010.

Griffis, T. J., Lee, X., Baker, J. M., Sargent, S. D., and King, J. Y.: Feasibility of quantifying ecosystem–atmosphere $C^{18}O^{16}O$ exchange using laser spectroscopy and the flux-gradient method, Agr. Forest Meteorol., 135, 44–60, 2005.

Griffis, T. J., Sargent, S. D., Baker, J. M., Lee, X., Tanner, B. D., Greene, J., Swiatek, E., and Billmark, K.: Direct measurement of biosphere-atmosphere isotopic CO_2 exchange using the eddy covariance technique, J. Geophys. Res., 113, D08304, doi:10.1029/2007JD009297, 2008.

Griffith, D. W. T., Deutscher, N. M., Caldow, C., Kettlewell, G., Riggenbach, M., and Hammer, S.: A Fourier transform infrared trace gas and isotope analyser for atmospheric applications, Atmos. Meas. Tech., 5, 2481–2498, doi:10.5194/amt-5-2481-2012, 2012.

Guillon, S., Pili, E., and Agrinie, P.: Using a laser-based CO_2 carbon isotope analyser to investigate gas transfer in geological media, Appl. Phys. B, 107, 449–457, 2012.

Hammer, S., Griffith, D. W. T., Konrad, G., Vardag, S., Caldow, C., and Levin, I.: Assessment of a multi-species in-situ FTIR for precise atmospheric greenhouse gas observations, Atmos. Meas. Tech. Discuss., 5, 3645–3692, doi:10.5194/amtd-5-3645-2012, 2012.

Kammer, A., Tuzson, B., Emmenegger, L., Knohl, A., Mohn, J., and Hagedorn, F.: Application of a quantum cascade laser-based spectrometer in a closed chamber system for real-time $\delta^{13}C$ and $\delta^{18}O$ measurements of soil-respired CO_2, Agr. Forest Meteorol., 151, 39–48, 2011.

Kerstel, E. and Gianfrani, L.: Advances in laser-based isotope ratio measurements: selected applications, Appl. Phys. B, 92, 439–449, 2008.

Koch, P. L.: Isotopic study of the biology of modern and fossil vertebrates, in: Stable Isotopes in Ecology and Environmental Science, 2nd Edn., edited by: Michener, R. and Lajtha, K., Blackwell Publishing Ltd, Oxford, UK, doi:10.1002/9780470691854.ch5, 2008.

Lee, X., Sargent, S., Smith, R., and Tanner, B.: In-situ measurement of water vapor $^{18}O/^{16}O$ isotope ratio for atmospheric and ecological applications, J. Atmos. Ocean. Tech., 22, 555–565, 2005.

McAlexander, I., Rau, G. H., Liem, J., Owano, T., Fellers, R., Baer, D., and Gupta, M.: Deployment of a carbon isotope ratiometer for the monitoring of CO_2 sequestration leakage, Anal. Chem., 83, 6223–6229, 2011.

Mohn, J., Zeeman, M. J., Werner, R. A., Eugster, W., and Emmenegge, L.: Continuous field measurements of $\delta^{13}C - CO_2$ and trace gases by FTIR spectroscopy, Isot. Environ. Healt. S., 44, 241–251, 2008.

Title Page

Abstract	Introduction
Conclusions	References
Tables	Figures

|◄ | ►|

◄ | ►

Back | Close

Full Screen / Esc

Printer-friendly Version

Interactive Discussion

Nara, H., Tanimoto, H., Tohjima, Y., Mukai, H., Nojiri, Y., Katsumata, K., and Rella, C. W.: Effect of air composition (N_2, O_2, Ar, and H_2O) on CO_2 and CH_4 measurement by wavelength-scanned cavity ring-down spectroscopy: calibration and measurement strategy, Atmos. Meas. Tech., 5, 2689–2701, doi:10.5194/amt-5-2689-2012, 2012.

Pataki, D. E., Ehleringer, J. R., Flanagan, L. B., Yakir, D., Bowling, D. R., Still, C. J., Buchmann, N., Kaplan, J. O., and Berry, J. A.: The application and interpretation of Keeling plots in terrestrial carbon cycle research, Global Biogeochem. Cy., 17, 1022, doi:10.1029/2001GB001850, 2003.

Pataki, D. E., Xu, T., Luo, Y. Q., and Ehleringer, J. R.: Inferring biogenic and anthropogenic carbon dioxide sources across an urban to rural gradient, Oecologia, 152, 307–322, 2007.

Rella, C. W.: Accurate stable carbon isotope ratio measurements in humid gas streams using the Picarro $\delta^{13}CO_2$ G2101-i gas analyzer, White Paper of Picarro Inc, Sunnyvale, CA, 1–13, 2012.

Rella, C. W., Chen, H., Andrews, A. E., Filges, A., Gerbig, C., Hatakka, J., Karion, A., Miles, N. L., Richardson, S. J., Steinbacher, M., Sweeney, C., Wastine, B., and Zellweger, C.: High accuracy measurements of dry mole fractions of carbon dioxide and methane in humid air, Atmos. Meas. Tech. Discuss., 5, 5823–5888, doi:10.5194/amtd-5-5823-2012, 2012.

Santos, E., Wagner-Riddle, C., Lee, X., Warland, J., Brown, S., Staebler, R., Bartlett, P., and Kim, K.: Use of the isotope flux ratio approach to investigate the $C^{18}O^{16}O$ and $^{13}CO_2$ exchange near the floor of a temperate deciduous forest, Biogeosciences, 9, 2385–2399, doi:10.5194/bg-9-2385-2012, 2012.

Sturm, P., Eugster, W., and Knohl, A.: Eddy covariance measurements of CO_2 isotopologues with a quantum cascade laser absorption spectrometer, Agr. Forest Meteorol., 152, 73–82, 2012.

Vogel, F. R., Huang, L., Ernst, D., Giroux, L., Racki, S., and Worthy, D. E. J.: Evaluation of a cavity ring-down spectrometer for in-situ observations of $^{13}CO_2$, Atmos. Meas. Tech. Discuss., 5, 6037–6058, doi:10.5194/amtd-5-6037-2012, 2012.

Wada, R., Pearce, J. K., Nakayama, T., Matsumi, Y., Hiyama, T., Inoue, G., and Shibata, T.: Observation of carbon and oxygen isotopic compositions of CO_2 at an urban site in Nagoya using Mid-IR laser absorption spectroscopy, Atmos. Environ., 45, 1168–1174, 2011.

Title Page

Abstract | Introduction

Conclusions | References

Tables | Figures

◀ | ▶

◀ | ▶

Back | Close

Full Screen / Esc

Printer-friendly Version

Interactive Discussion

Welp, L., Lee, X., Griffis, T., Wen, X. F., Xiao, W., Li, S. G., Sun, X. M., Hu, Z. M., Martin, M. V., and Huang, J. P.: A meta-analysis of water vapor deuterium-excess in the mid-latitude atmospheric surface layer, Global Biogeochemical Cy., 26, GB3021, doi:10.1029/2011GB004246, 2012.

Wen, X. F., Sun, X. M., Zhang, S. C., Yu, G. R., Sargent, S. D., and Lee, X.: Continuous measurement of water vapor D/H and $^{18}O/^{16}O$ isotope ratios in the atmosphere, J. Hydrol., 349, 489–500, 2008.

Wen, X. F., Lee, X., Sun, X. M., Wang, J. L., Tang, Y. K., Li, S. G., and Yu, G. R.: Intercomparison of four commercial analyzers for water vapor isotope measurement, J. Atmos. Ocean. Tech., 29, 235–247, 2012.

Werle, P.: Accuracy and precision of laser spectrometers for trace gas sensing in the presence of optical fringes and atmospheric turbulence. Appl. Phys. B, 102, 313–329, 2011.

Werner, C., Schnyder, H., Cuntz, M., Keitel, C., Zeeman, M. J., Dawson, T. E., Badeck, F.-W., Brugnoli, E., Ghashghaie, J., Grams, T. E. E., Kayler, Z. E., Lakatos, M., Lee, X., Máguas, C., Ogée, J., Rascher, K. G., Siegwolf, R. T. W., Unger, S., Welker, J., Wingate, L., and Gessler, A.: Progress and challenges in using stable isotopes to trace plant carbon and water relations across scales, Biogeosciences, 9, 3083–3111, doi:10.5194/bg-9-3083-2012, 2012.

Wingate, L., Ogée, J., Burlett, R., Alexandre, B., Devaux, M., Grace, J., Loustau, D., and Gessler, A.: Photosynthetic carbon isotope discrimination and its relationship to the carbon isotope signals of stem, soil and ecosystem respiration, New Phytol., 188, 576–589, 2010.

Title Page

Abstract | Introduction

Conclusions | References

Tables | Figures

◀ | ▶

◀ | ▶

Back | Close

Full Screen / Esc

Printer-friendly Version

Interactive Discussion

Table 1. Inter-comparison of four δ^{13}C calibration methods. In the case of Method 1–2, one of the three standard gases (Std 1, Std 2 and Std 3) was treated as the target of measurement and the other two were used for calibration. In the case of Method 3, Std 3 was used in conjunction of either Std 1 or Std 2 as the calibration pair. In the case of Method 4, Std 3 was used to calibrate the measurement of Std 1 and Std 2. Standard deviations are for hourly measurements ($n = 24$). CO_2 mixing ratios are in ppm and delta measurements are in ‰.

| | Standard | [CO_2] | True δ^{13}C | Measured δ^{13}C | δ^{13}C error | | | |
					Method 1	Method 2	Method 3	Method 4
Picarro	Std 1	361.25	−8.909	−10.70 ± 0.51	−0.01 ± 0.65	0.04 ± 0.58	0.26 ± 0.34	0.43 ± 0.39
	Std 2	398.76	−8.652	−10.68 ± 0.52	0.00 ± 0.29	−0.02 ± 0.29	−0.19 ± 0.32	0.19 ± 0.33
	Std 3	436.41	−10.134	−12.35 ± 0.50	0.00 ± 0.52	0.04 ± 0.58	–	–
Los Gatos	Std 1	361.25	−8.909	−13.24 ± 0.89	−0.03 ± 0.23	0.13 ± 0.20	0.61 ± 0.09	1.37 ± 0.11
	Std 2	398.76	−8.652	−13.73 ± 0.84	0.01 ± 0.10	−0.06 ± 0.10	−0.49 ± 0.05	0.62 ± 0.11
	Std 3	436.41	−10.134	−15.83 ± 0.90	−0.02 ± 0.18	0.13 ± 0.20	–	–

Table 2. Keeling mixing line analysis of ambient measurement in Beijing during DOY 103-110 in 2012. The regression was made using the calibrated $\delta^{13}C$ against the reciprocal of the calibrated CO_2 concentration. Gas standard Std 1 and Std 3 were used for Methods 1–3 and Std 3 was used for Method 4.

		Method 1	Method 2	Method 3	Method 4
Picarro (00:00–24:00)	Slope	6133.3 ± 421.3	6143.7 ± 424.6	8564.9 ± 882.2	6133.0 ± 437.4
	Intercept	-23.85 ± 1.00	-23.88 ± 1.02	-29.62 ± 2.13	-23.86 ± 1.05
	R^2	0.83	0.83	0.61	0.82
Picarro (22:00–04:00)	Slope	6185.0 ± 824.7	6862.5 ± 823.5	1143.8 ± 2343.7	6569.9 ± 926.3
	Intercept	-25.53 ± 1.99	-25.64 ± 1.99	-36.54 ± 5.65	-24.97 ± 2.23
	R^2	0.88	0.88	0.65	0.84
Los Gatos (00:00–24:00)	Slope	5336.7 ± 333.0	4795.1 ± 330.4	3533.1 ± 128.5	9123.6 ± 349.9
	Intercept	-21.85 ± 0.79	-20.62 ± 0.79	-18.02 ± 0.31	-30.53 ± 0.83
	R^2	0.86	0.83	0.95	0.95
Los Gatos (22:00–04:00)	Slope	6154.6 ± 635.9	5626.7 ± 646.8	3818.9 ± 261.8	1003.6 ± 648.9
	Intercept	-23.81 ± 1.52	-22.60 ± 1.55	-18.70 ± 0.63	-32.70 ± 1.56
	R^2	0.91	0.89	0.95	0.97
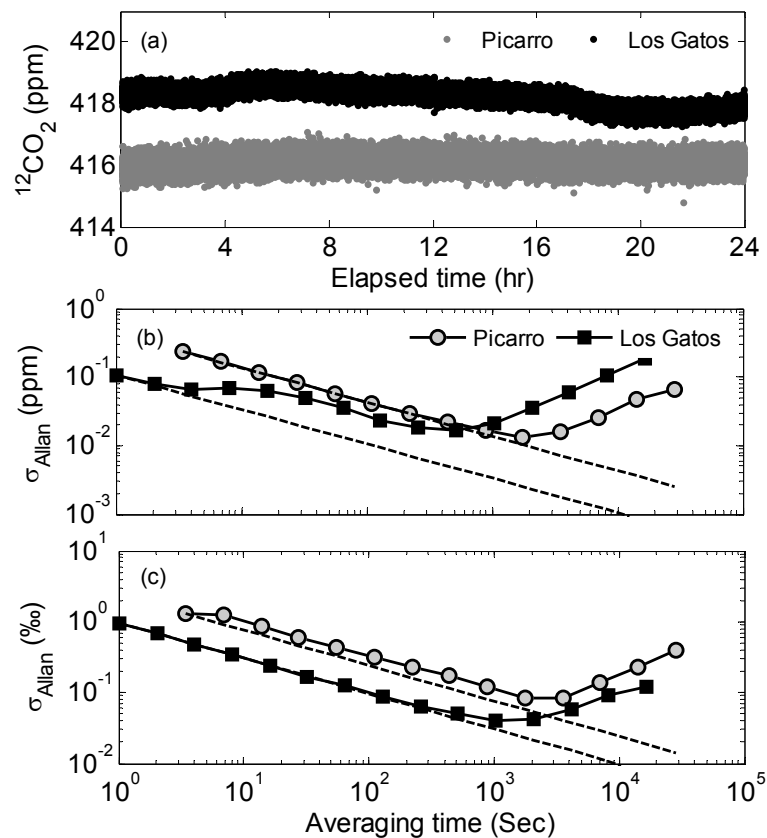
Fig. 1. Time series of the **(a)** $^{12}CO_2$ concentration and Allan deviation of the **(b)** $^{12}CO_2$ concentration and **(c)** $\delta^{13}C$ for the Picarro and the Los Gatos analyzer. The dashed lines show the expected behavior of the Allan deviation versus time for random noises.
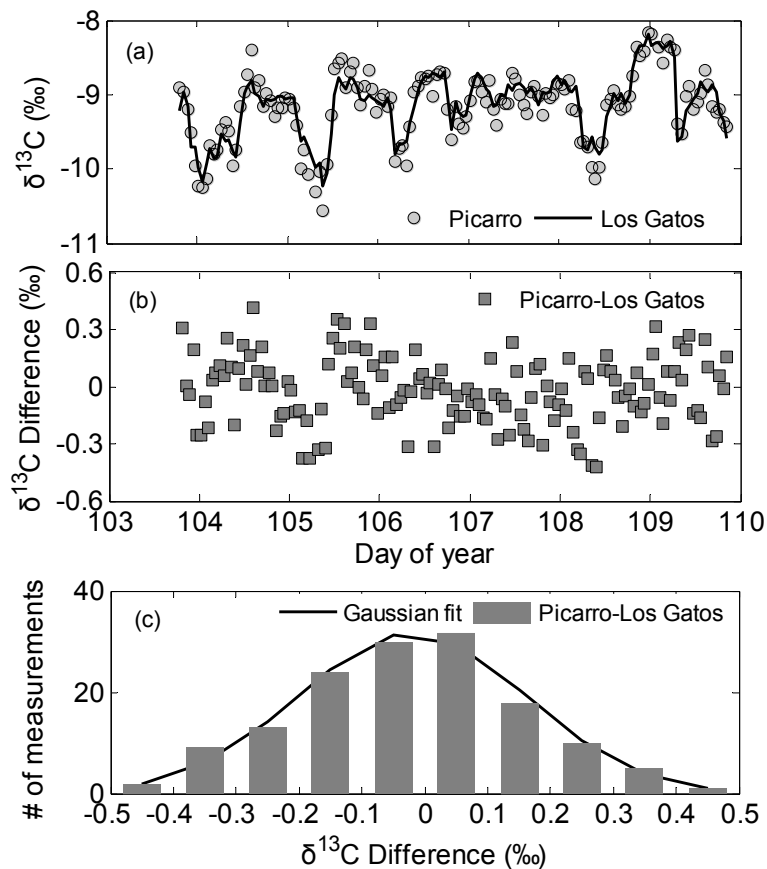
Fig. 2. Time variations of **(a)** hourly atmospheric $\delta^{13}C$ in Beijing during DOY 103–110 in 2012, **(b)** difference between the Picarro and the Los Gatos analyzers, and **(c)** histogram of the differences. Here Method 1 was used for calibration.
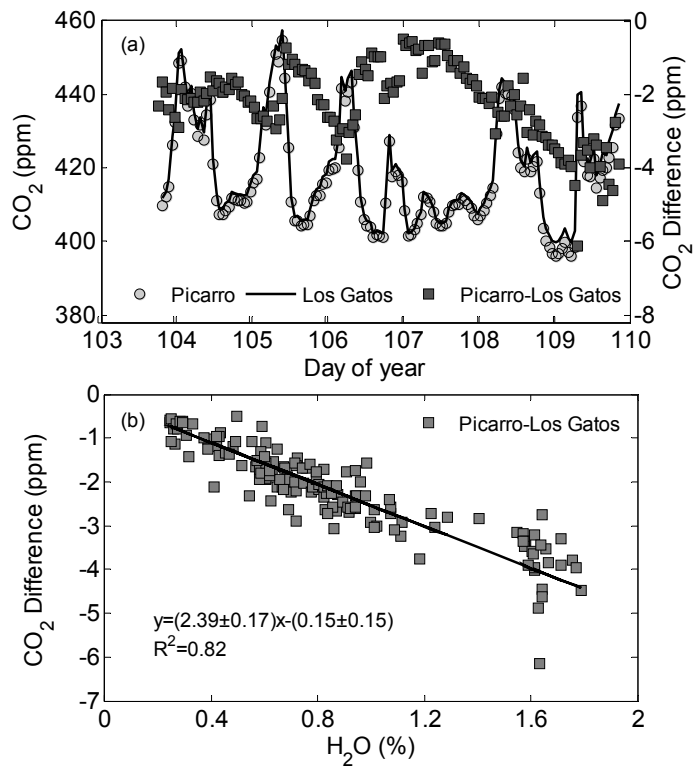
Fig. 3. (a) Same as for Fig. 2a except for hourly atmospheric CO_2 concentration and **(b)** dependence of their difference on the H_2O concentration.

Full Screen / Esc

Printer-friendly Version

Interactive Discussion
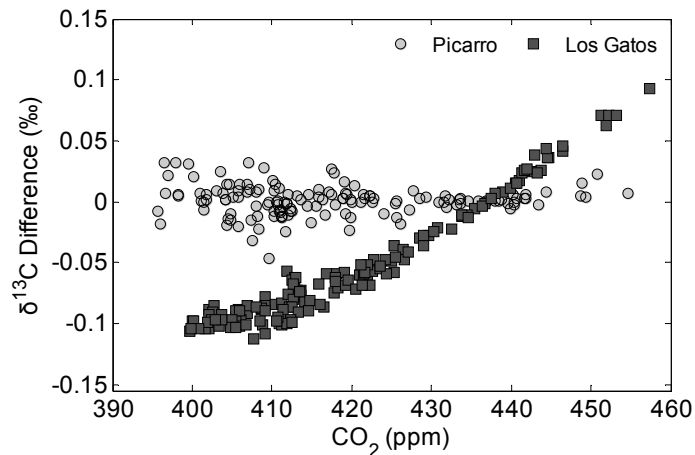
Fig. 4. Dependence of the difference in atmospheric $\delta^{13}C$ between Method 1 and Method 2 on the CO_2 concentration.
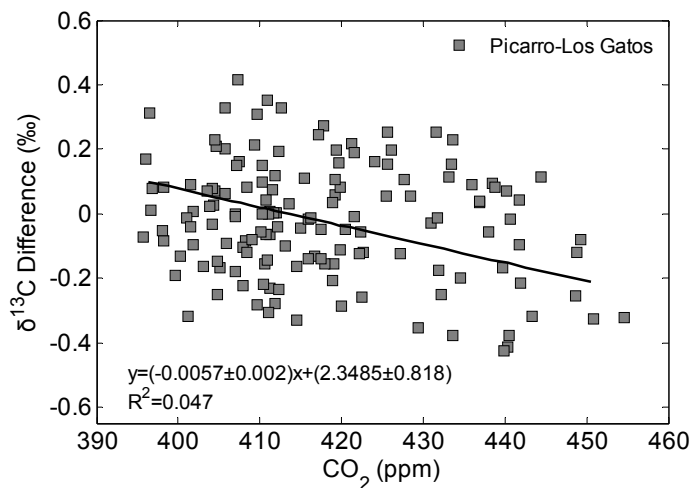
Fig. 5. Dependence of the difference in atmospheric $\delta^{13}C$ between the two analyzers on the CO_2 concentration. Here Method 1 was used for calibration.
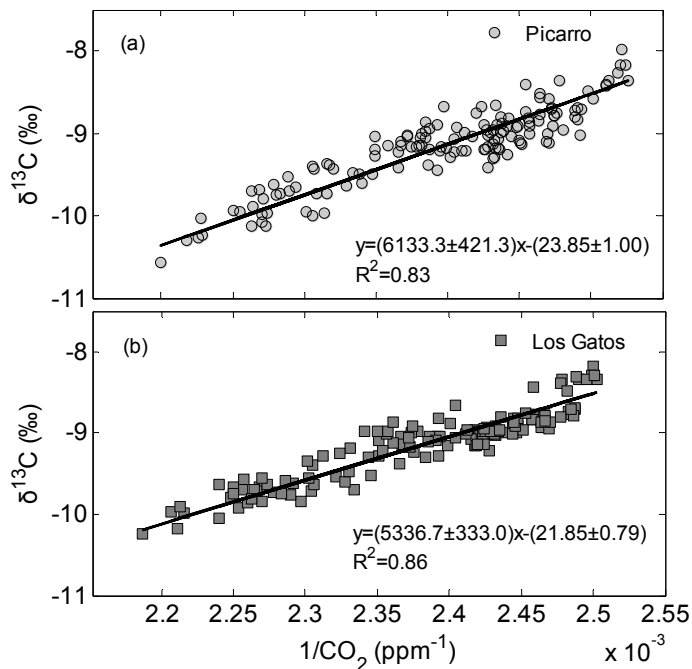
Fig. 6. Keeling plot of the calibrated atmospheric δ^{13}C against the reciprocal of the calibrated CO_2 concentration for **(a)** the Picarro and **(b)** the Los Gatos analyzers. Both daytime and night-time data were used. Calibration was made with Method 1.
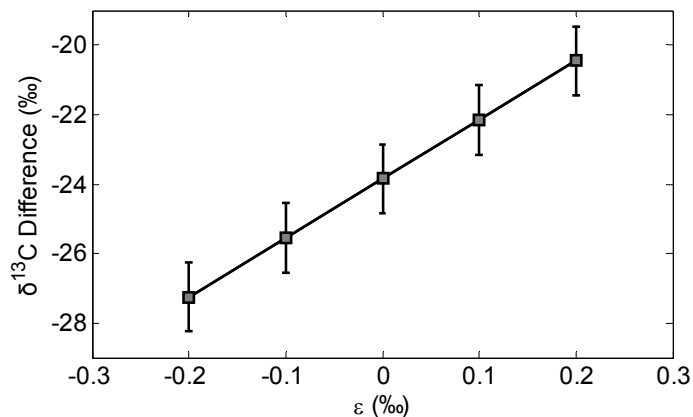
Fig. 7. The relationship of the intercept of the Keeling plot to the parameter specifying the concentration dependence behavior (Eqs. 13–15). Error bars indicate the 95 % confidence bound.